

## Pion decay constant at finite temperature and density

A. Barducci

*Dipartimento di Fisica, Università di Firenze, I-50125 Firenze, Italy  
and Istituto Nazionale di Fisica Nucleare, Sezione di Firenze, I-50125 Firenze, Italy*

R. Casalbuoni

*Dipartimento di Fisica, Università di Lecce, I-73100 Lecce, Italy  
and Istituto Nazionale di Fisica Nucleare, Sezione di Lecce, I-73100 Lecce, Italy*

S. De Curtis

*Istituto Nazionale di Fisica Nucleare, Sezione di Firenze, I-50125 Firenze, Italy*

R. Gatto

*Département de Physique Théorique, Université de Genève, CH-1211 Genève 4, Switzerland*

G. Pettini

*Istituto Nazionale di Fisica Nucleare, Sezione di Firenze, I-50125 Firenze, Italy*

(Received 3 May 1990)

The pion decay constant and the fermionic bilinear condensate at finite temperature and density are evaluated in the whole region of broken chirality by using the composite-operator approach to QCD. The critical exponents around the tricritical point (separating first-order from second-order phase transitions) are determined by general thermodynamical arguments.

### I. INTRODUCTION

The study of QCD at finite temperature and density has recently attracted much interest. Among the domains of applications are high-energy heavy-ion collisions<sup>1</sup> and the physics of the early Universe.<sup>2</sup> Both deconfinement and chiral-symmetry restoration are expected to take place when the temperature  $T$  and/or the chemical potential  $\lambda$  are large. The nature of the transition from the hadronic phase at low temperatures and densities to the quark-gluon phase for large temperatures and/or densities is not yet entirely known. It is not known whether a single transition occurs or separate transitions take place for deconfinement and chiral symmetry.

The theoretical considerations so far are based on discussion of order parameters which cover extreme and opposite ranges. The thermally averaged Polyakov loop is suitable in the limit of infinite quark masses to describe the transition from the confined to the nonconfined phase. At the other extreme, in the limit of vanishing quark masses, the quark-antiquark bilinears, thermally averaged, are the typical order parameters for chiral-symmetry transition.

We do not know which set of order parameters is suitable to describe the phase structure of real QCD with physical quarks and gluons. Also, no symmetry (or symmetries) beyond the chiral symmetry for the limiting case of vanishing quark masses suggest itself as convenient to identify the different phases in terms of its patterns of breaking. In a recent paper<sup>3</sup> we have suggested a heuristic argument indicating that, for zero density, the critical

temperature for chiral transition  $T_c$  coincides with that for deconfinement  $T_d$ .

In the present article we shall deal exclusively with the chiral transition, concentrating on the thermally averaged quark bilinears, in the presence of a chemical potential, as order parameters for chirality.

The formal tool of the present analysis will be a composite-operator formalism at finite temperature and density developed in previous works.<sup>4</sup> The formalism is based on an effective action for composite operators.<sup>5</sup>

The application of the formalism to QCD with light flavors has led<sup>4</sup> to a phase diagram on the  $(\lambda, T)$  plane where the phase of broken chiral symmetry is separated from the symmetric one by a line consisting of two pieces which join at a tricritical point  $t \equiv (\lambda_t, T_t)$ . The transition is second order for  $\lambda < \lambda_t$  and it becomes first order for  $\lambda > \lambda_t$ .

The pion decay constant at fixed  $\lambda$  and  $T$ ,  $f_\pi(\lambda, T)$ , is an essential parameter of the theory, certainly relevant to the description of the chiral properties and, as suggested,<sup>3</sup> also playing a role in the description of confinement. We have already discussed the  $T$  dependence of  $f_\pi(\lambda, T)$  for  $\lambda=0$ ,<sup>6</sup> in the whole range of temperatures up to  $T_c$ , within our composite-operator formalism.

An important feature of the calculation of  $f_\pi(T)$ , as it will be for the calculation to be presented here for both  $T$  and  $\lambda$  finite, is the agreement of the result near the critical points to that predicted from thermodynamical arguments on critical exponents. These exponents follow from general considerations, near the different critical points and near the tricritical point, along the full  $(\lambda, T)$  critical regions of the phase diagram. We find the typical

behavior coming from the Landau mean-field theory. Crucial to this behavior is the complete absence of infrared divergences in the expansion of our effective potential around the second-order phase transition line and around the tricritical point.

So far only the low-temperature expansion for  $\lambda=0$  is known within a sufficient generality.<sup>7</sup> Its extrapolation up to the critical point, always at  $\lambda=0$ , would however fail to obey the universality rules and it is therefore doubtful. Our results agree with the low- $T$  expansion. In addition, they satisfy the universality rules at the critical points.

## II. FORMALISM

We shall essentially extend the work made in Ref. 6 to the general case of finite temperature and finite chemical potential  $\lambda$ . This is made through the generalization of the Feynman rules for pion amplitudes given in Ref. 5 to finite temperature and density. We remind the reader that the quark propagator is written as (here and in the following we shall use Euclidean notation)

$$S^{-1}(p) = i\hat{p} - \Sigma(p) - m, \quad (2.1)$$

where  $\Sigma(p)$  is  $T$  and  $\lambda$  dependent, and  $m$  is the quark current mass. We will work in the  $m \rightarrow 0$  limit. Similarly to Ref. 4 we assume

$$\Sigma(p) = \chi(T, \lambda) \frac{\mu^3}{p^2 + \mu^2}, \quad (2.2)$$

where  $\mu$  is a scale parameter determined phenomenologically to be  $\simeq 282$  MeV,<sup>5</sup> and  $\chi(T, \lambda)$  is a variational parameter which is evaluated by minimizing the effective potential given in Ref. 4. This parameter is related to the fermion condensate by

$$\langle \bar{\psi}\psi \rangle_{T, \lambda} = \frac{3\mu^3}{2\pi^2} c(T, \lambda) \chi(T, \lambda), \quad (2.3)$$

where  $c(T, \lambda)$  is defined, as in Ref. 4, in terms of the gauge coupling constant  $g^2(T, \lambda)$  which runs with  $T$  and  $\lambda$  according to

$$c(T, \lambda) = \frac{2\pi^2}{g^2(T, \lambda)} \equiv c_0 + c_1(T, \lambda), \quad (2.4)$$

$$f_\pi^2(T, \lambda) = 12 \sum_{n=-\infty}^{\infty} (-)^n \int \frac{d^4 p}{(2\pi)^4} \frac{\Sigma(p) \left[ \Sigma(p) - 2p_0^2 \frac{\partial \Sigma(p)}{\partial p^2} \right]}{[p^2 + \Sigma^2(p)]^2} e^{in(p_0 - i\lambda)/T}. \quad (2.10)$$

## III. PION DECAY CONSTANT AT FINITE TEMPERATURE AND DENSITY

To evaluate  $f_\pi(T, \lambda)$  it is convenient to separate in Eq. (2.10) the  $n=0$  contribution and write

$$f_\pi^2(T, \lambda) = \bar{f}_\pi^2(T, \lambda) + \hat{f}_\pi^2(T, \lambda), \quad (3.1)$$

where

$$\bar{f}_\pi^2(T, \lambda) = \frac{3}{(2\pi)^2} \int_0^\infty dp^2 p^2 \frac{\Sigma^2(p) - \frac{1}{2} p^2 \Sigma(p) \frac{\partial \Sigma(p)}{\partial p^2}}{[p^2 + \Sigma^2(p)]^2} \quad (3.2)$$

where (assuming, for definiteness, three light flavors)

$$c_0 = \frac{2\pi^2}{g^2} = \frac{9}{8} \ln \left[ \frac{\mu^2}{\Lambda_{\text{QCD}}^2} \right], \quad (2.5)$$

$$c_1(T, \lambda) = \frac{9}{8} \ln \left[ 1 + \xi \frac{T^2}{\mu^2} + \zeta \frac{\lambda^2}{\mu^2} \right], \quad (2.6)$$

and  $g^2$  is the value of the gauge coupling constant evaluated at the scale  $\mu$ . The constant  $c_0$  is fixed to be  $\simeq 0.554$  (see Ref. 4) and it corresponds to  $\Lambda_{\text{QCD}} \simeq 220$  MeV. The parameters  $\xi$  and  $\zeta$ , introduced to account for the evolution of  $g^2(T, \lambda)$  with the temperature and the chemical potential, will be left for the moment as free parameters. The expectation value in Eq. (2.3) is the thermal average in the presence of a chemical potential, defined, for a generic operator  $A$ , as

$$\langle A \rangle_{T, \lambda} \equiv \frac{\text{Tr}(e^{-(H-\lambda N)/T} A)}{\text{Tr}(e^{-(H-\lambda N)/T})}, \quad (2.7)$$

where  $N$  is the particle number operator.

The effects due to finite temperature and chemical potential can be taken into account in the Feynman rules by simply modifying the integration over the intermediate states according to

$$\begin{aligned} \int \frac{d^4 p}{(2\pi)^4} f(p) &\rightarrow T \sum_{n=-\infty}^{\infty} \int \frac{d^3 \mathbf{p}}{(2\pi)^3} f((2n+1)\pi T + i\lambda, \mathbf{p}) \\ &= \sum_{n=-\infty}^{\infty} (-)^n \int \frac{d^4 p}{(2\pi)^4} f(p) e^{in(p_0 - i\lambda)/T}. \end{aligned} \quad (2.8)$$

This substitution corresponds to the imaginary-time formalism after using Poisson's formula.

To evaluate the pion decay constant as a function of  $T$  and  $\lambda$ , we define  $f_\pi(T, \lambda)$  through the relation

$$\langle 0 | \partial^\mu J_\mu^5 | \pi \rangle_{T, \lambda} = m_\pi^2(T, \lambda) f_\pi(T, \lambda). \quad (2.9)$$

We then evaluate the matrix element as done in Ref. 6 by using the Feynman rules we have discussed. We find

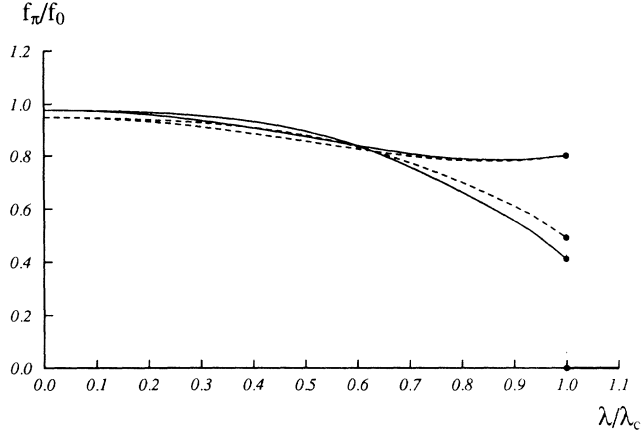


FIG. 1. Plot of  $f_\pi/f_0$  vs  $\lambda/\lambda_c$  at  $T \approx 42$  MeV. The solid lines correspond to  $\xi=0.6$  [ $\zeta=0.9$  (upper line),  $\zeta=0.1$  (lower line), corresponding to  $\lambda_c \approx 165$  and  $290$  MeV, respectively]. The dashed lines correspond to  $\xi=1.5$  [ $\zeta=0.9$  (upper line),  $\zeta=0.1$  (lower line), corresponding to  $\lambda_c \approx 160$  and  $280$  MeV, respectively]. The terms “upper” and “lower” refer to the relative positions of the lines at  $\lambda=\lambda_c$ .

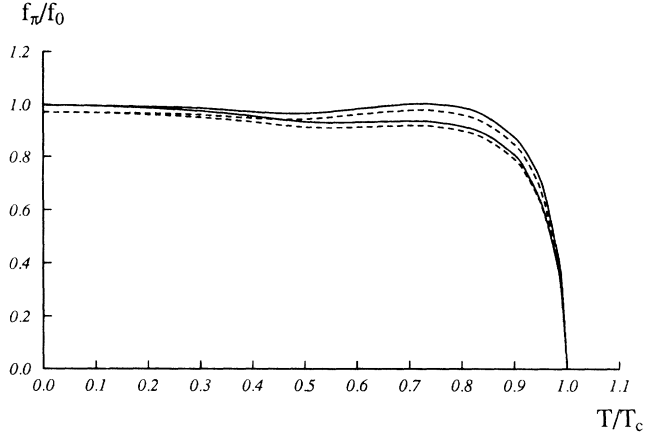


FIG. 2. Plot of  $f_\pi/f_0$  vs  $T/T_c$  at  $\lambda \approx 42$  MeV. The solid lines correspond to  $\zeta=0.1$  [ $\xi=0.6$  (upper line),  $\xi=1.5$  (lower line), corresponding to  $T_c \approx 105$  and  $94$  MeV, respectively]. The dashed lines correspond to  $\zeta=0.9$  [ $\xi=0.6$  (upper line),  $\xi=1.5$  (lower line), corresponding to  $T_c \approx 103$  and  $92$  MeV, respectively].

and, by the same manipulations as in Ref. 6,

$$\hat{f}_\pi^2(T, \lambda) = \frac{3\mu^2}{\pi^2} \chi^2(T, \lambda) \frac{d}{d\chi^2} \sum_{i=1}^3 \left[ \frac{dz_i}{d\chi^2} (1-z_i) \int_0^\infty dy y^2 \frac{1-2y^2-3z_i}{\sqrt{y^2+z_i}} \frac{1}{1+\exp[(\mu\sqrt{y^2+z_i}+\lambda)/T]} + (\lambda \rightarrow -\lambda) \right], \quad (3.3)$$

where  $z_i$  are the roots (changed in sign) of the cubic equation

$$x^3 + 2x^2 + x + \chi^2 = 0. \quad (3.4)$$

Notice that the only dependence on  $T$  and  $\lambda$  of  $\bar{f}_\pi^2(T, \lambda)$  comes from the value of  $\chi(T, \lambda)$  corresponding to the minimum of the effective potential. Also the dependence of  $f_\pi^2(T, \lambda)$  on the parameters  $\xi$  and  $\zeta$  comes only through  $\chi(T, \lambda)$ . One possible choice for  $\xi$  comes by re-

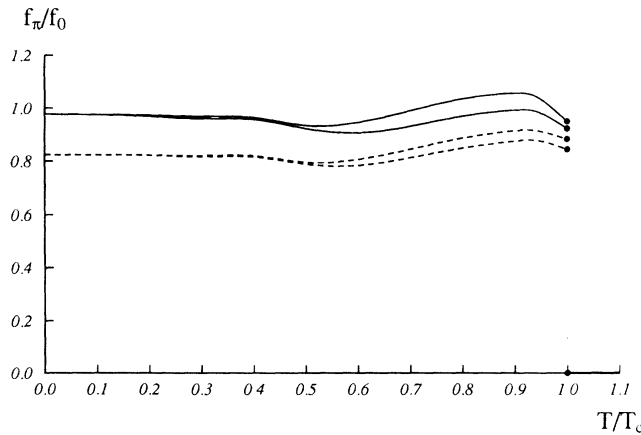


FIG. 3. Plot of  $f_\pi/f_0$  vs  $T/T_c$  at  $\lambda \approx 113$  MeV. The solid lines correspond to  $\zeta=0.1$  [ $\xi=0.6$  (upper line),  $\xi=1.5$  (lower line), corresponding to  $T_c \approx 85$  and  $76$  MeV, respectively]. The dashed lines correspond to  $\zeta=0.9$  [ $\xi=0.6$  (upper line),  $\xi=1.5$  (lower line), corresponding to  $T_c \approx 69$  and  $64$ , respectively].

quiring that  $f_\pi$  at  $\lambda=0$  coincides at low  $T$  with the low-temperature expansion of Ref. 7. This gives  $\xi \approx 1$  (Ref. 6). As far as  $\zeta$ , a possible indication comes from Ref. 8 which gives, for three light flavors,  $\zeta/\xi \approx 0.15$ .

The behavior of  $f_\pi(T, \lambda)$  is illustrated in Figs. 1–3. In Fig. 1 we give  $f_\pi/f_0$  [where  $f_0 = f_\pi(0, 0)$  which, with our choice of the parameters  $c_0$  and  $\mu$ , is  $\approx 91$  MeV] at fixed  $T$  before the tricritical point as a function of  $\lambda/\lambda_c$ . The graph illustrates the first-order character of the phase transition in the chemical potential for various values of the parameters  $\xi$  and  $\zeta$ . In Figs. 2 and 3 we give  $f_\pi/f_0$  at fixed  $\lambda$  before and after the tricritical point as a function of  $T/T_c$  for various choices of the parameters  $\xi$  and  $\zeta$ . For the calculation of the tricritical point see Sec. IV. In Table I we give the coordinates of the tricritical points for some values of  $\xi$  and  $\zeta$ .

#### IV. BEHAVIOR AROUND THE TRICRITICAL POINT

To study the behavior of the theory around the tricritical point we recall from Ref. 4 the expression for the effective potential

TABLE I.  $(\lambda_c, T_c)$  in MeV for some values of  $\xi$  and  $\zeta$ .

$\xi \backslash \zeta$	0.0	0.6	1.0	1.5
0.1	(82, 107)	(78, 96)	(76, 92)	(75, 87)
0.6	(80, 101)	(77, 92)	(75, 88)	(74, 84)
0.9	(79, 97)	(76, 90)	(74, 86)	(73, 83)
1.2	(78, 94)	(75, 88)	(74, 84)	(73, 81)

$$V = \frac{9\mu^4}{4\pi^2} \bar{V}, \tag{4.1}$$

$$\begin{aligned} \bar{V}(\chi, T, \lambda) = & \frac{c(T, \lambda)}{3} \chi^2 - \frac{1}{2} \int_0^\infty dx x \ln \left[ 1 + \frac{\chi^2}{x^3 + 2x^2 + x} \right] \\ & - 4 \frac{T}{\mu} \sum_{i=1}^3 \int_0^\infty dx x^2 [\ln(1 + \exp\{-[\mu\sqrt{(x^2+z_i)} + \lambda]/T\}) + (\lambda \rightarrow -\lambda)]. \end{aligned} \tag{4.2}$$

Here, as in Refs. 4 and 6, we have neglected terms which do not depend on  $\chi$ , but which may still depend on  $T$  and  $\lambda$ . These terms play no role in the considerations made in Refs. 4 and 6 and in the present context (they are, however, important from the thermodynamical point of view). In Ref. 4 we have shown that the effective potential (4.2) gives rise, in general, to a phase diagram in the  $(\lambda, T)$  plane (see Fig. 4), having one line of second-order phase transitions ( $L_{II}$ ), and a second line of first-order phase transitions ( $L_I$ ), which join at a tricritical point  $t \equiv (\lambda_t, T_t)$ . These two lines divide the  $(\lambda, T)$  plane in two disconnected regions corresponding to the chiral-broken and to the chiral-symmetric phases. Along  $L_{II}$  up to the tricritical point the absolute minimum of the effective potential is at  $\chi=0$ ; therefore, we can study the theory around  $t$  by expanding  $\bar{V}$  for small values of  $\chi$ . To study the behavior at the points of  $L_I$  close to the tricritical point, it is necessary to expand  $\bar{V}$  up to the sixth order in  $\chi$  (Ref. 9). From this expansion it will be possible to determine the critical exponents for  $\chi$  and consequently for the condensate and for  $f_\pi$ .

When expanding the effective potential, one may expect to encounter problems related to the property of  $\chi$  to be proportional to the order parameter of the chiral-symmetry breaking. In fact, in the  $\chi \rightarrow 0$  limit, the fermions in the theory become massless, and infrared divergences might show up in the coefficients of the expansion of the effective potential. For instance, by taking  $\bar{V}$  at zero temperature and zero chemical potential, one sees immediately that the fourth derivative at the origin is infrared divergent. In fact, in the  $\chi \rightarrow 0$  limit, this term

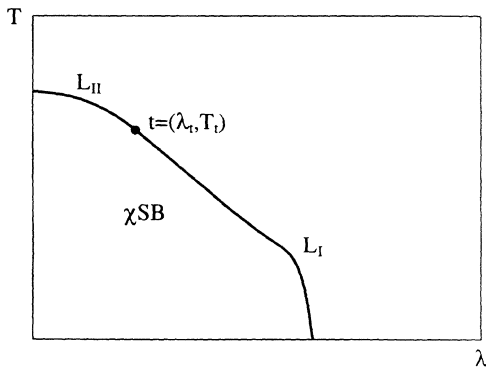


FIG. 4. Phase diagram in the  $(\lambda, T)$  plane showing the line of the first-order phase transitions ( $L_I$ ), the line of the second-order phase transitions ( $L_{II}$ ), and the tricritical point  $t \equiv (\lambda_t, T_t)$ .

gives rise to a contribution  $-\frac{1}{4}\chi^4 \ln \chi^2$ . However, the full calculation shows that the fourth derivative is free of infrared divergences. The same happens for the sixth derivative. As a consequence we get a definite power series up to the sixth order of the effective potential:

$$\begin{aligned} \bar{V}(\chi, T, \lambda) = & \bar{V}(0, T, \lambda) + a_2(T, \lambda) \chi^2 \\ & + a_4(T, \lambda) \chi^4 + a_6(T, \lambda) \chi^6 + \dots \end{aligned} \tag{4.3}$$

The critical line  $L_{II}$  is determined by the equation

$$a_2(T, \lambda) = 0, \quad a_4(T, \lambda) > 0, \tag{4.4}$$

and the coordinates of the tricritical point are solutions of the equations

$$a_2(T, \lambda) = a_4(T, \lambda) = 0. \tag{4.5}$$

The coordinates of the tricritical point change slowly with  $\xi$  and  $\zeta$  (at least in the physically interesting region) as shown in Table I.

As a side issue we notice that at points close to  $L_{II}$  but far from  $t$ , we can, for instance, at fixed  $\lambda$ , expand  $a_2$  around the critical temperature. Since at these points  $a_4 \neq 0$ , we can limit the expansion (4.3) to the fourth order. Then applying the same procedure as in Ref. 6, we easily see that the critical exponent for  $\chi$  (and consequently for the condensate and for  $f_\pi$ ) is  $\frac{1}{2}$ .

Let us expand  $a_2(T, \lambda)$  and  $a_4(T, \lambda)$  around the tricritical point

$$a_2(T, \lambda) \simeq a_2^T(\xi, \zeta) \left[ 1 - \frac{T}{T_t} \right] + a_2^\lambda(\xi, \zeta) \left[ 1 - \frac{\lambda}{\lambda_t} \right], \tag{4.6}$$

$$a_4(T, \lambda) \simeq a_4^T(\xi, \zeta) \left[ 1 - \frac{T}{T_t} \right] + a_4^\lambda(\xi, \zeta) \left[ 1 - \frac{\lambda}{\lambda_t} \right].$$

Direct calculation shows that  $a_6(T_t, \lambda_t) \equiv a_6^t(\xi, \zeta) > 0$ . In Figs. 5-7 we have plotted the coefficients  $a_2^T, a_2^\lambda, a_4^T, a_4^\lambda, a_6^t$  vs  $\xi$  for various values of  $\zeta$ .

It is convenient, for the following discussion, to map the critical lines on the  $(a_2, a_4)$  plane. This is done in Fig. 8. It is easy to show that in the broken phase, around the tricritical point, the absolute minimum of the effective potential has the expression

$$\chi = \left[ \frac{-a_4 + (a_4^2 - 3a_2a_6)^{1/2}}{3a_6} \right]^{1/2}. \tag{4.7}$$

To determine the critical exponents we have only to use

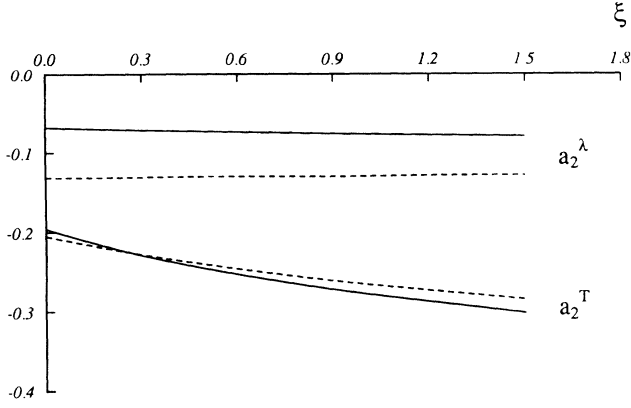


FIG. 5. The coefficients  $a_2^T$  and  $a_2^\lambda$  vs  $\xi$  for  $\zeta=0.1$  (solid line) and  $\zeta=1.2$  (dashed line).

(4.6) in (4.7) and specify the direction by which one approaches the tricritical point. For instance, if we fix  $\lambda=\lambda_t$ , we find

$$\begin{aligned} \chi(T) &\simeq \left[ -\frac{a_2^T}{3a_6^t} \right]^{1/4} \left[ 1 - \frac{T}{T_t} \right]^{1/4} \\ &\equiv a_\chi^\lambda(\xi, \zeta) \left[ 1 - \frac{T}{T_t} \right]^{1/4}. \end{aligned} \quad (4.8)$$

Analogously at  $T=T_t$  we get

$$\begin{aligned} \chi(\lambda) &\simeq \left[ -\frac{a_2^\lambda}{3a_6^t} \right]^{1/4} \left[ 1 - \frac{\lambda}{\lambda_t} \right]^{1/4} \\ &\equiv a_\chi^T(\xi, \zeta) \left[ 1 - \frac{\lambda}{\lambda_t} \right]^{1/4}. \end{aligned} \quad (4.9)$$

More generally, we see from (4.7) that, except the case  $a_2=0$ , the dominant term is given by

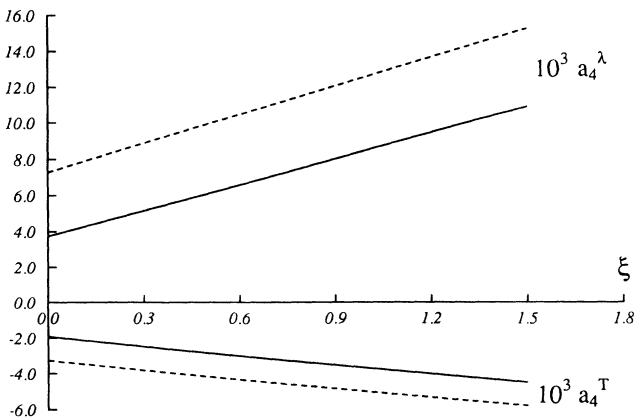


FIG. 6. The coefficients  $a_4^T$  and  $a_4^\lambda$  vs  $\xi$  for  $\zeta=0.1$  (solid line) and  $\zeta=1.2$  (dashed line).

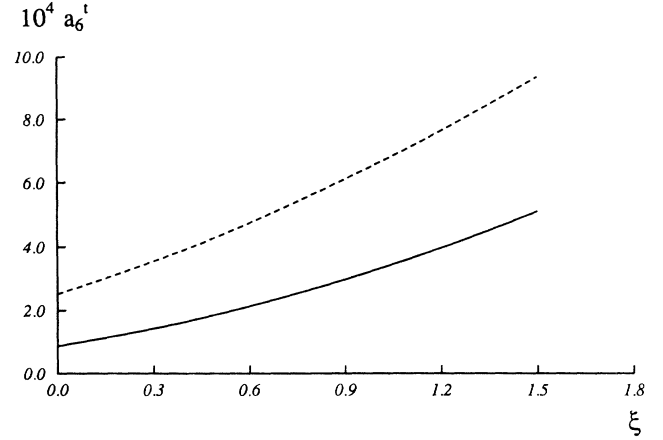


FIG. 7. The coefficient  $a_6^t$  vs  $\xi$  for  $\zeta=0.1$  (solid line) and  $\zeta=1.2$  (dashed line).

$$\chi(T, \lambda) \simeq \left[ \frac{|a_2|}{3a_6^t} \right]^{1/4} \quad (4.10)$$

showing that the critical exponent is always  $\frac{1}{4}$  along any direction around the tricritical point, the exception being the direction  $a_2=0$  and  $a_4 < 0$ , for which we find

$$\chi \simeq \left[ -\frac{2}{3} \frac{a_4}{a_6^t} \right]^{1/2}. \quad (4.11)$$

Finally, if we move along  $L_I$  near to the tricritical point, we can evaluate the discontinuity of  $\chi$ . We find

$$\Delta\chi = \left[ \frac{a_2}{a_6^t} \right]^{1/4} \quad (4.12)$$

showing that the gap goes to zero at the tricritical point.

From Eq. (2.3) we see that the critical exponents of the fermion condensate are the same as those of  $\chi(T, \lambda)$ . For the two particular directions considered in Eqs. (4.8) and

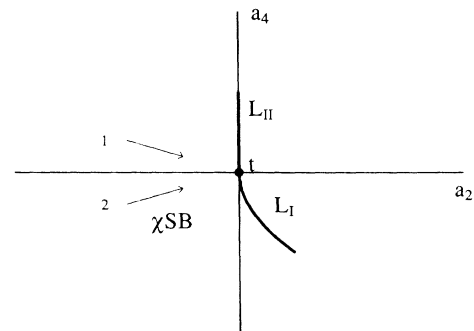


FIG. 8. The mapping of the critical lines on the plane  $(a_2, a_4)$ . The directions 1 and 2 correspond in the  $(\lambda, T)$  plane to paths at fixed  $T$  and  $\lambda$ , respectively.

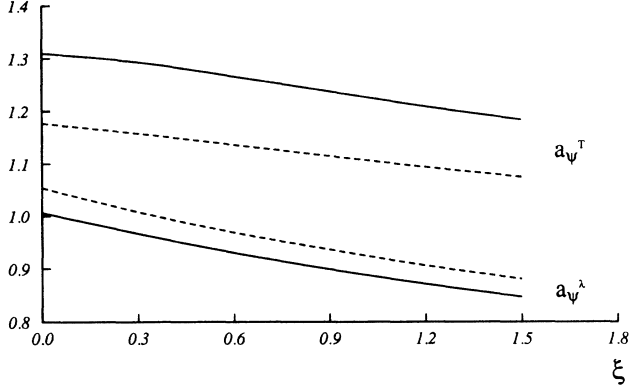


FIG. 9. The coefficients  $a_\psi^T$  and  $a_\psi^\lambda$  vs  $\xi$  for  $\zeta=0.1$  (solid line) and  $\zeta=1.2$  (dashed line).

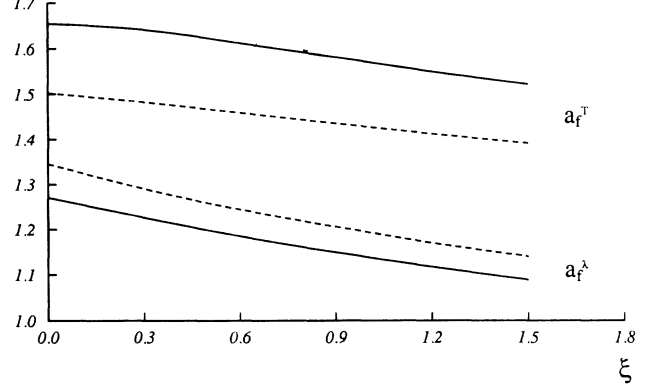


FIG. 10. The coefficients  $a_f^T$  and  $a_f^\lambda$  vs  $\xi$  for  $\zeta=0.1$  (solid line) and  $\zeta=1.2$  (dashed line).

(4.9) we find  $(\langle \bar{\psi}\psi \rangle)_0 = \langle \bar{\psi}\psi \rangle_{T=0, \lambda=0}$

$$\frac{\langle \bar{\psi}\psi \rangle_{T, \lambda_t}}{\langle \bar{\psi}\psi \rangle_0} \simeq a_\psi^\lambda(\xi, \zeta) \left[ 1 - \frac{T}{T_t} \right]^{1/4}, \quad (4.13)$$

$$\frac{\langle \bar{\psi}\psi \rangle_{T_t, \lambda}}{\langle \bar{\psi}\psi \rangle_0} \simeq a_\psi^T(\xi, \zeta) \left[ 1 - \frac{\lambda}{\lambda_t} \right]^{1/4}, \quad (4.14)$$

with

$$a_\psi^i(\xi, \zeta) = \frac{c(T_t, \lambda_t)}{c_0 \chi_0} a_\chi^i(\xi, \zeta), \quad i = \lambda, T, \quad (4.15)$$

where  $\chi_0 \simeq 4.06$  (see Ref. 4) is the minimum at zero temperature and chemical potential. In Fig. 9 we plot  $a_\psi^i$ ,  $i = \lambda, T$ , as functions of  $\xi$  for various values of  $\zeta$ .

Coming to the pion decay constant, we see from Eq. (2.10) that we can write

$$\frac{f_\pi(T, \lambda)}{f_0} = \chi(T, \lambda) G(T, \lambda, \chi(T, \lambda)) \quad (4.16)$$

and one can check that  $G(T_t, \lambda_t, 0)$  is regular (it is free of infrared divergences) and different from zero. It follows that the behavior of  $f_\pi(T, \lambda)$  around the tricritical point is the same as  $\chi(T, \lambda)$ . For the two particular directions considered in Eqs. (4.8) and (4.9) we find

$$\frac{f_\pi(T)}{f_0} \simeq a_f^\lambda(\xi, \zeta) \left[ 1 - \frac{T}{T_t} \right]^{1/4}, \quad (4.17)$$

$$\frac{f_\pi(\lambda)}{f_0} \simeq a_f^T(\xi, \zeta) \left[ 1 - \frac{\lambda}{\lambda_t} \right]^{1/4}, \quad (4.18)$$

with

$$a_f^i(\xi, \zeta) = a_\chi^i(\xi, \zeta) G(T_t, \lambda_t, 0), \quad i = \lambda, T. \quad (4.19)$$

The coefficients  $a_f^i(\xi, \zeta)$  are given as functions of  $\xi$ , for various values of  $\zeta$ , in Fig. 10.

## V. CONCLUSIONS

We have studied the pion decay constant in QCD at finite temperature and density. The calculations are carried out within a composite-operator formalism. Our previous work with the same formalism had given a QCD phase diagram in the plane of chemical potential  $\lambda$  and temperature  $T$  formed by a line for second-order phase transitions and a line for first-order phase transitions both joining at a tricritical point  $t \equiv (\lambda_t, T_t)$ . Universal thermodynamical arguments can be applied to study the behavior of  $f_\pi(T, \lambda)$  and of the chiral condensate  $\langle \bar{\psi}\psi \rangle_{T, \lambda}$  near the phase transitions and in particular near the tricritical point. Our calculations agree with predictions of such general arguments (critical exponents). Crucial is the absence of infrared divergence. In the general case our results follow from a two-step procedure, where the effective QCD potential is first minimized, to obtain the value of the chiral condensate. Then, such a condensate value is inserted into an approximate expression for  $f_\pi(T, \lambda)$ , which extends to finite  $\lambda$  and  $T$  the chiral expression for  $f_\pi(0, 0)$ , through generalization of Feynman-diagram techniques. The critical exponents have been explicitly evaluated around the tricritical point. Quantitatively our treatment is perhaps sufficiently adequate to deal with chiral effects and with the chiral transition. We have, however, to assume that (gluonic) effects, which are probably important for the deconfinement, do not essentially alter the result. Unfortunately lattice methods may not be useful to describe situations of nonzero densities, which on the other hand, are inevitably present in experimental situations. In this sense our formalism may remain for a long time irreplaceable to deal with nonzero chemical potential, but we hope that more complex calculations may soon allow for additional verifications of our results.

## ACKNOWLEDGMENTS

This work was partially supported by the Swiss National Foundation.

- <sup>1</sup>For general reviews and references see, H. Satz, H. J. Specht, and R. Stock, in *Quark Matter '87*, proceedings of the Sixth International Conference on Ultrarelativistic Nucleus-Nucleus Collisions, Munster, West Germany, 1987 [Z. Phys. C **38**, 1 (1988)]; M. Jacob, in *Quark Matter '88*, proceedings of the Seventh International Conference on Ultrarelativistic Nucleus-Nucleus Collisions, Lenox, Massachusetts, 1988, edited by G. Baym, P. Braun-Munzinger, and S. Nagamiya [Nucl. Phys. A**498**, 1 (1989)]; P. Carruthers and J. Rafelski, in *Hadronic Matter in Collision 1988*, Tucson, Arizona, 1988, edited by P. Carruthers and J. Rafelski (World Scientific, Singapore, 1989); E. V. Shuryak, *The QCD Vacuum, Hadrons and Superdense Matter* (Lecture Notes in Physics, Vol. 8) (World Scientific, Singapore, 1988); D. Gross, R. Pisarski, and L. Yaffe, Rev. Mod. Phys. **53**, 43 (1981); J. Cleymans, R. V. Gavai, and E. Suhonen, Phys. Rep. **130**, 217 (1986); L. McLerran, Rev. Mod. Phys. **58**, 1021 (1986); F. Karsch, Z. Phys. C **38**, 147 (1988).
- <sup>2</sup>For reviews and references see A. D. Linde, Rep. Prog. Phys. **42**, 389 (1979); B. Sinha and S. Raha, in *Physics and Astrophysics of Quark-Gluon Plasma*, proceedings of the International Conference, Bombay, India, 1988, edited by B. Sinha and S. Raha (World Scientific, Singapore, 1989).
- <sup>3</sup>A. Barducci, R. Casalbuoni, S. De Curtis, R. Gatto, and G. Pettini, Phys. Lett. B (to be published).
- <sup>4</sup>A. Barducci, R. Casalbuoni, S. De Curtis, R. Gatto, and G. Pettini, Phys. Lett. B **231**, 463 (1989); Phys. Rev. D **41**, 1610 (1990).
- <sup>5</sup>A. Barducci, R. Casalbuoni, S. De Curtis, D. Dominici, and R. Gatto, Phys. Rev. D **38**, 238 (1988).
- <sup>6</sup>A. Barducci, R. Casalbuoni, S. De Curtis, R. Gatto, and G. Pettini, Phys. Lett. B **240**, 429 (1990).
- <sup>7</sup>P. Binetruy and M. K. Gaillard, Phys. Rev. D **32**, 931 (1985); J. Gasser and H. Leutwyler, Phys. Lett. B **184**, 83 (1987); **188**, 477 (1987).
- <sup>8</sup>O. K. Kalashnikov, Z. Phys. C **39**, 427 (1988); A. Cabo, O. K. Kalashnikov, and E. Kh. Veliev, Nucl. Phys. B**299**, 367 (1988).
- <sup>9</sup>See, for example, K. Huang, *Statistical Mechanics*, 2nd ed. (Wiley, New York, 1987).